# Nanoparticle

# Representative nanoparticle compositions and sizes

| Particle composition | Available particle size [nm] | |
|---|---|---|
| Metals | | |
| | Au | 2–150 |
| | Ag | 1–180 |
| | Pt | 1–20 |
| | Cu | 1–150 |
| Semiconductors | | |
| | CdX (X = S, Se, Te) | 1–20 |
| | ZnX (X = S, Se, Te) | 1–20 |
| | PbS | 2–18 |
| | $TiO_2$ | 3–50 |
| | ZnO | 1–30 |
| | GaAs, InP | 1–15 |
| | Ge | 6–30 |
| Magnetic | | |
| | $Fe_3O_4$ | 6–40 |
| Polymer | | |
| | Many compositions | 50–1000 |

# Size- and shape-dependent light scattering property

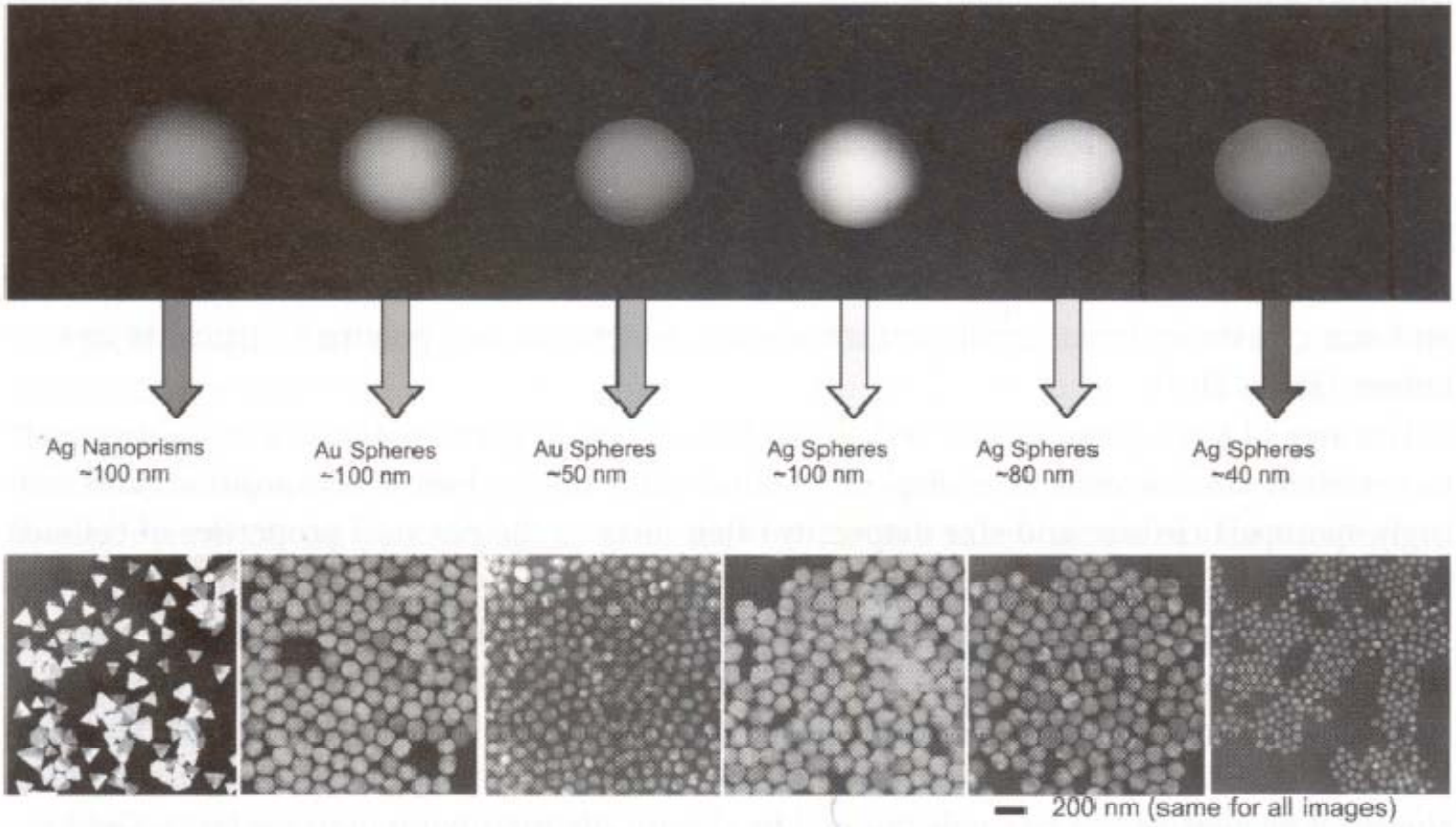


**Figure 19.1** Size- and shape-dependent light scattering by representative silver and gold nanoparticles with corresponding transmission electron microscopic (TEM) images of the particles.

# Quantum dots yield size-tunable emission.

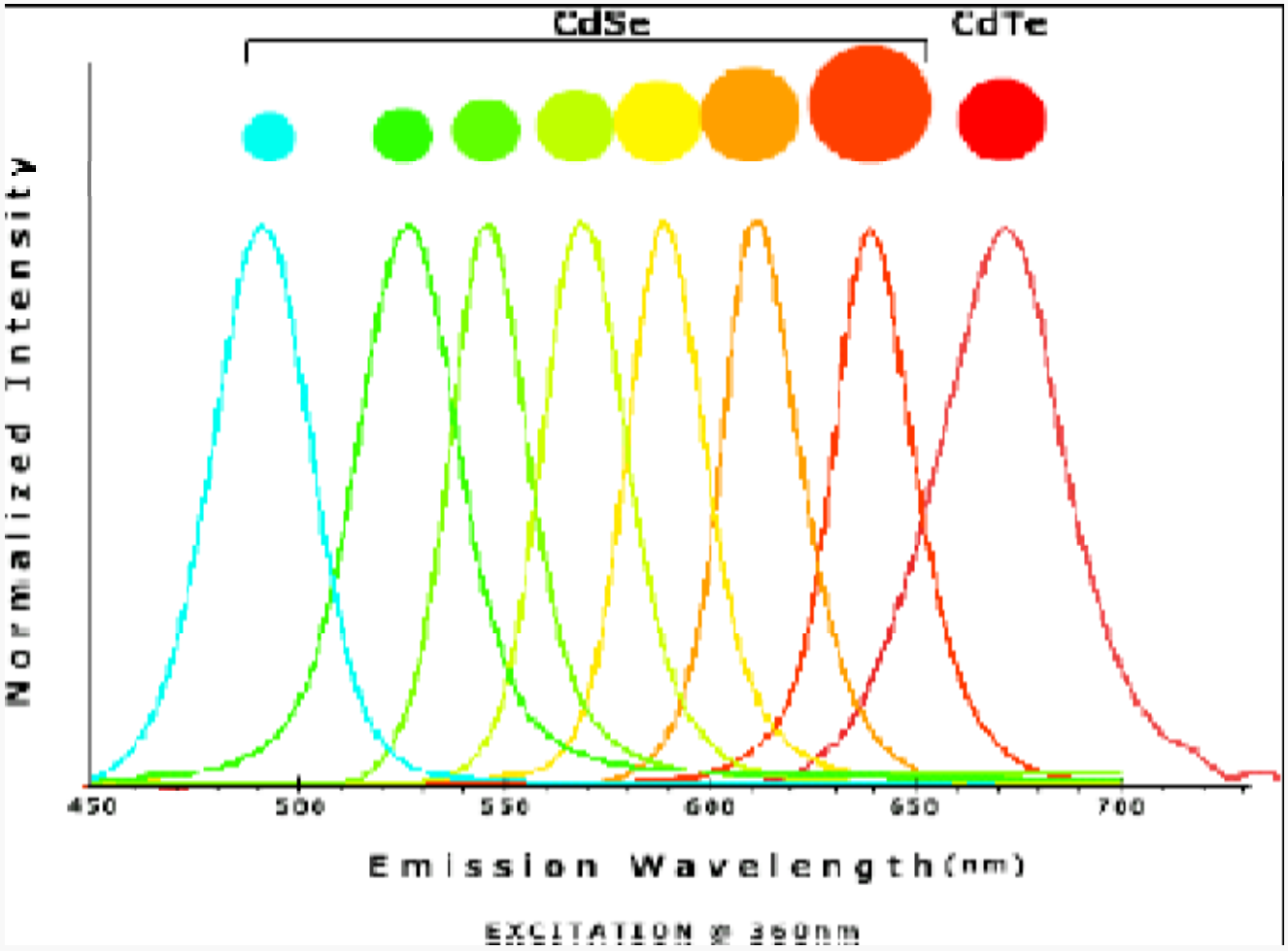

# Emission colors of CdSe/ZnS core/Shell Quantum dots

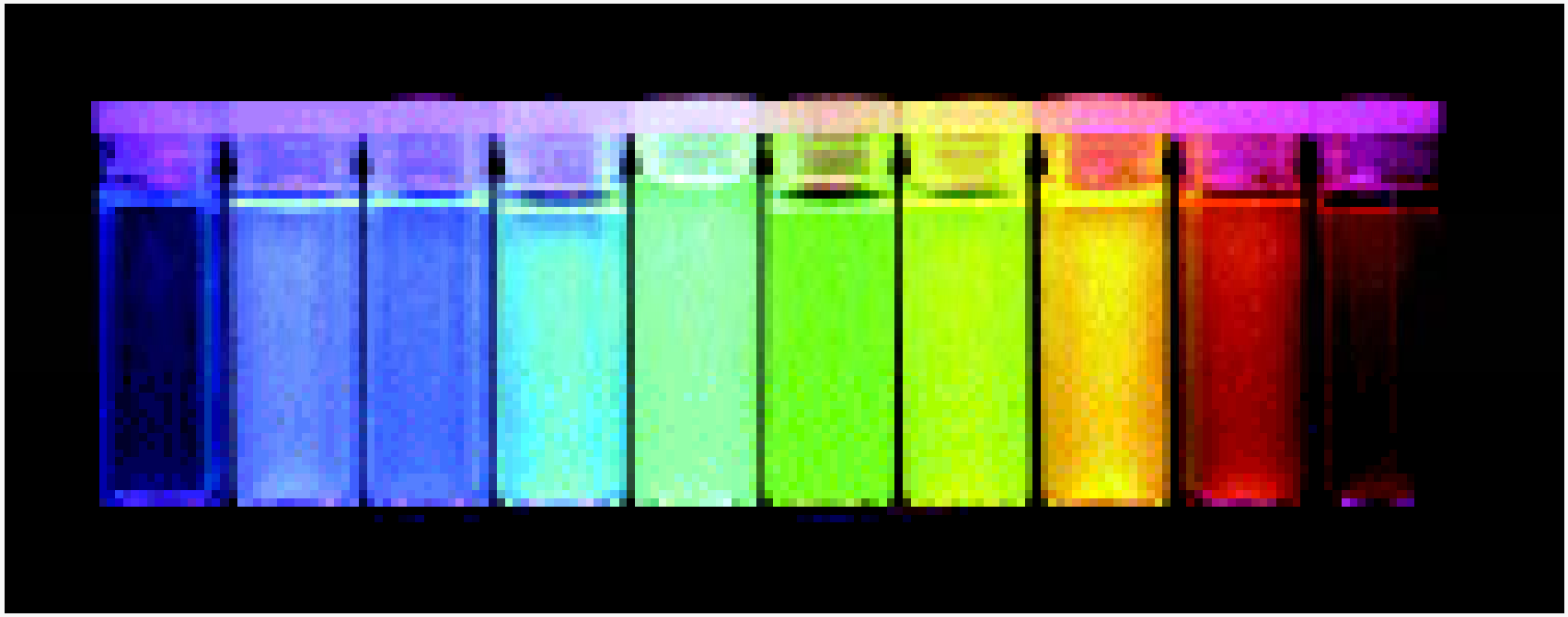

# DNA-functionalized Gold Nanoparticles

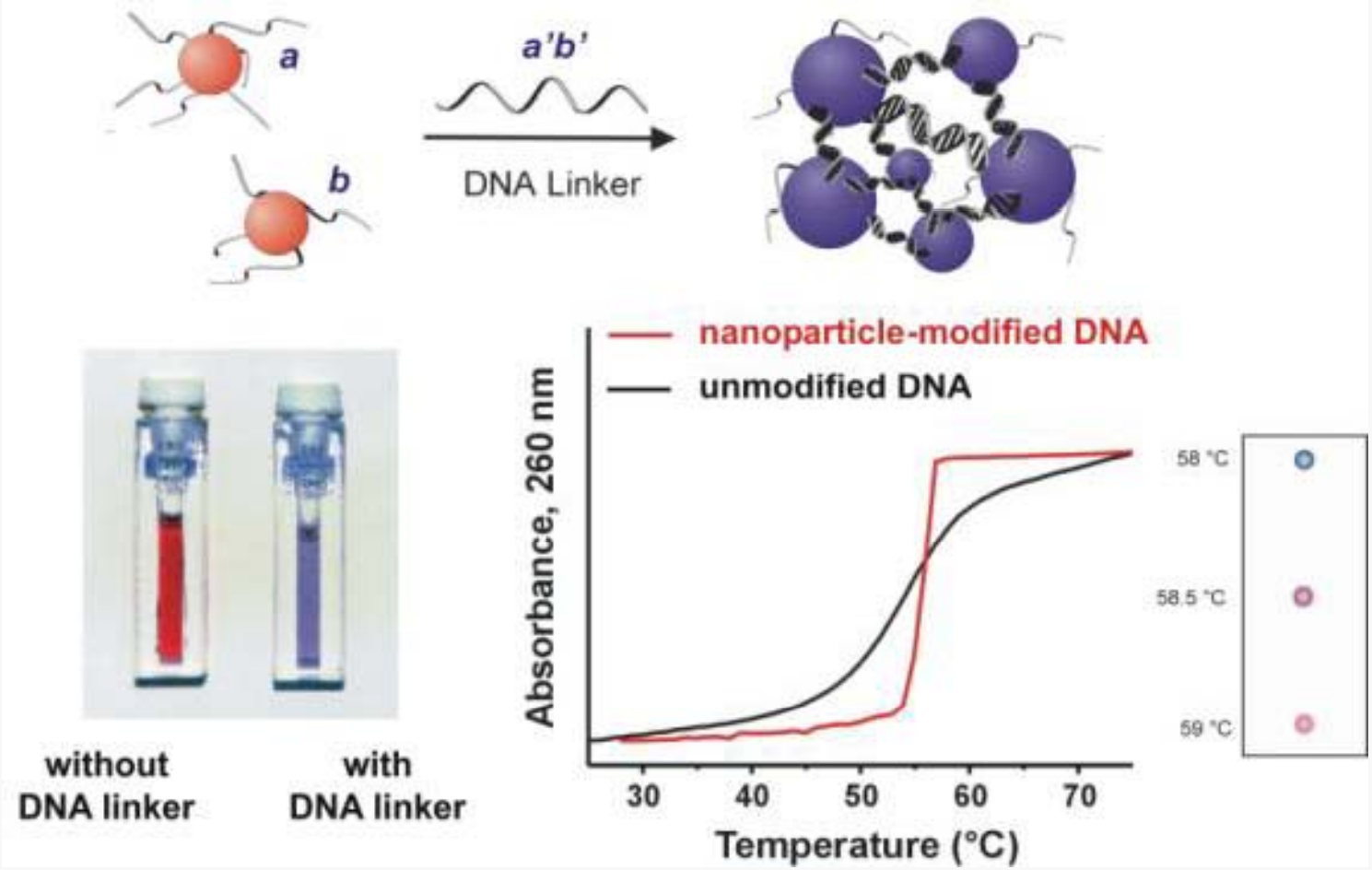


Thermal denaturation profiles


**Figure 19.3** Homogeneous single-nucleotide polymorphism (SNP) discrimination using DNA–nanoparticle probes. The sharp thermal denaturation profiles for gold nanoparticle probes allows for SNP detection. The Northwestern spot test is shown in which samples of the aggregate mixture are spotted to a reverse-phase silica plate at a given temperature permanently recording the hybridization status.

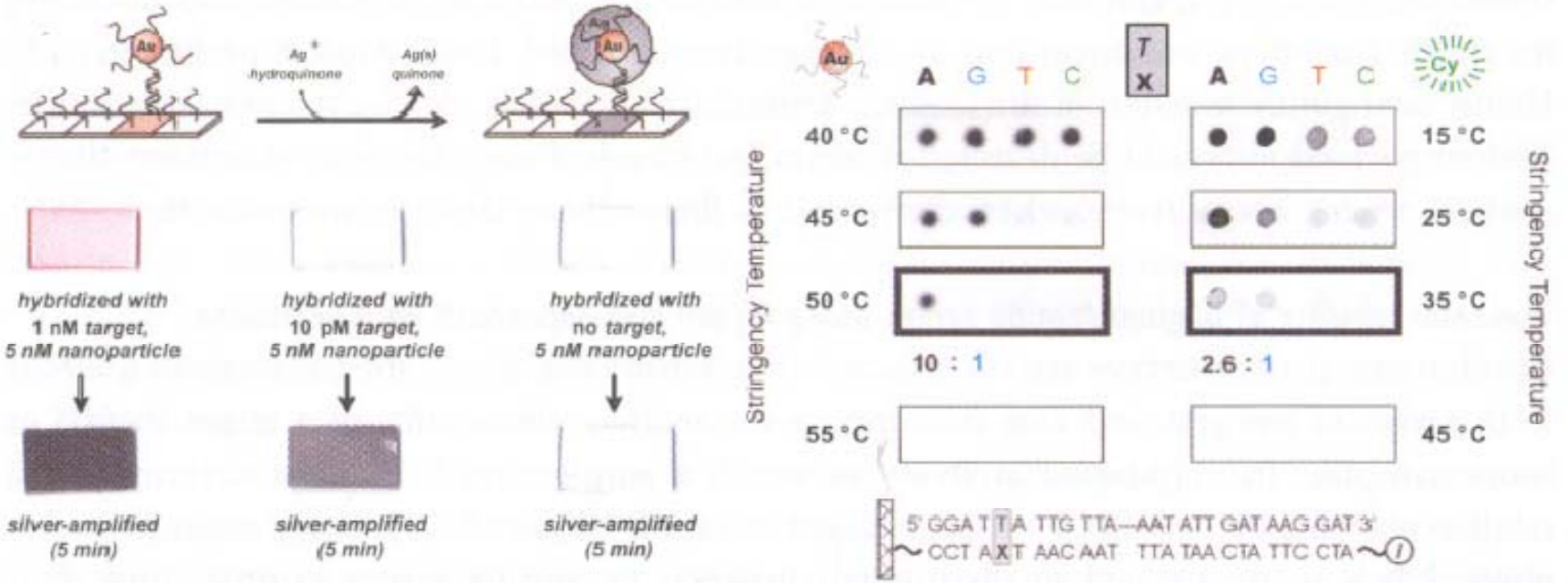


**Figure 19.4** Scanometric chip-based DNA detection sandwich assay using silver amplification of the detection signal. The scanometric DNA detection scheme is depicted on the left. A direct SNP detection/discrimination comparison of DNA-nanoparticles versus organic fluorophore labeling probes is shown on the right. The DNA-nanoparticle system is shown here to have a selective advantage of approximately 4:1.

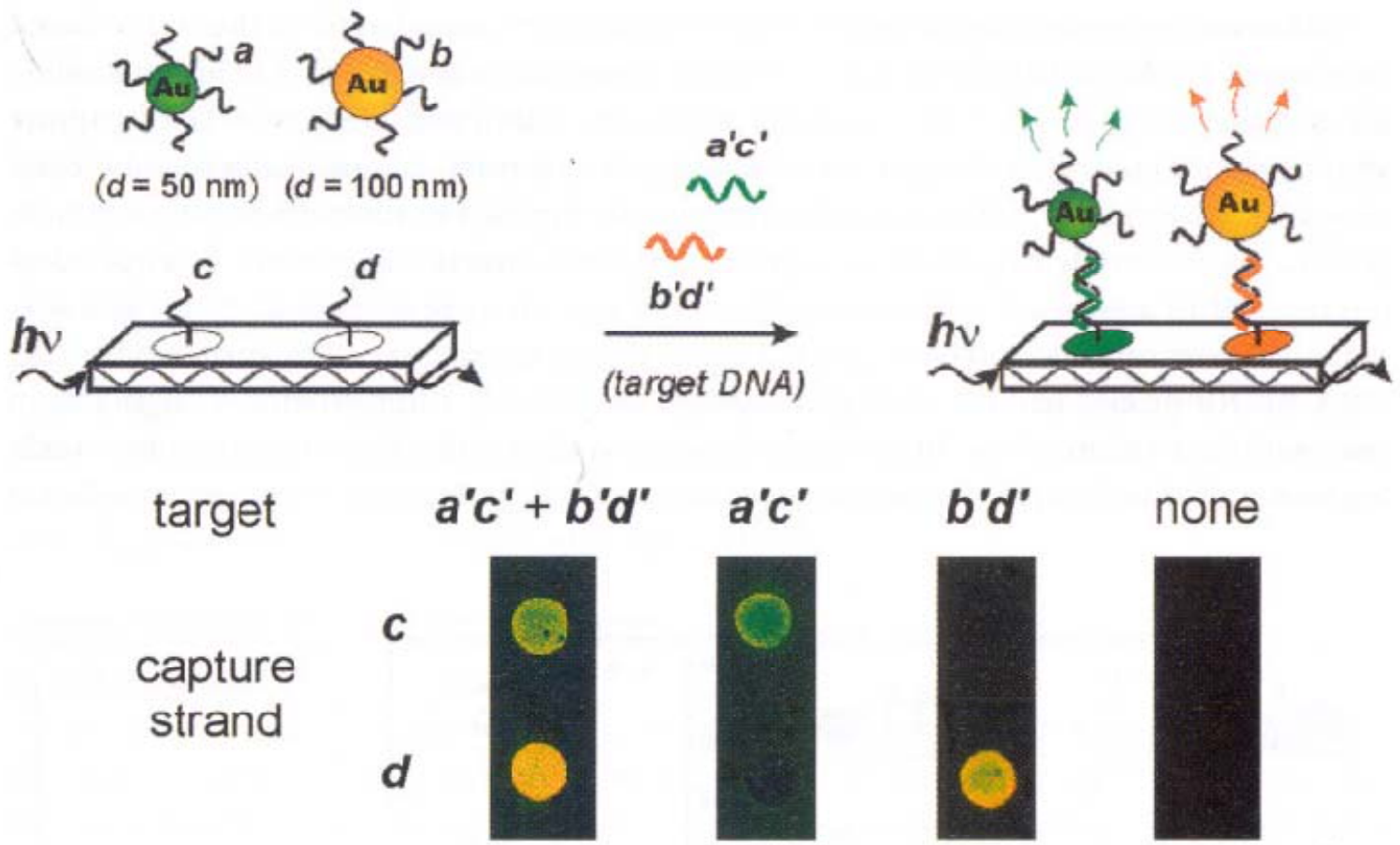


**Figure 19.5** Two-color DNA sandwich assay using light scattering from different diameter gold nanoparticle probes (a and b) specific for a given target (a'c' and b'd', respectively). When the target sequence is present and hybridizes with the appropriate chip-immobilized capture strand (c and d), the nanoparticle probes are bound to the surface. Evanescent illumination of the chip surface and dark-field visualization allows for the detection of specific hybridization events.

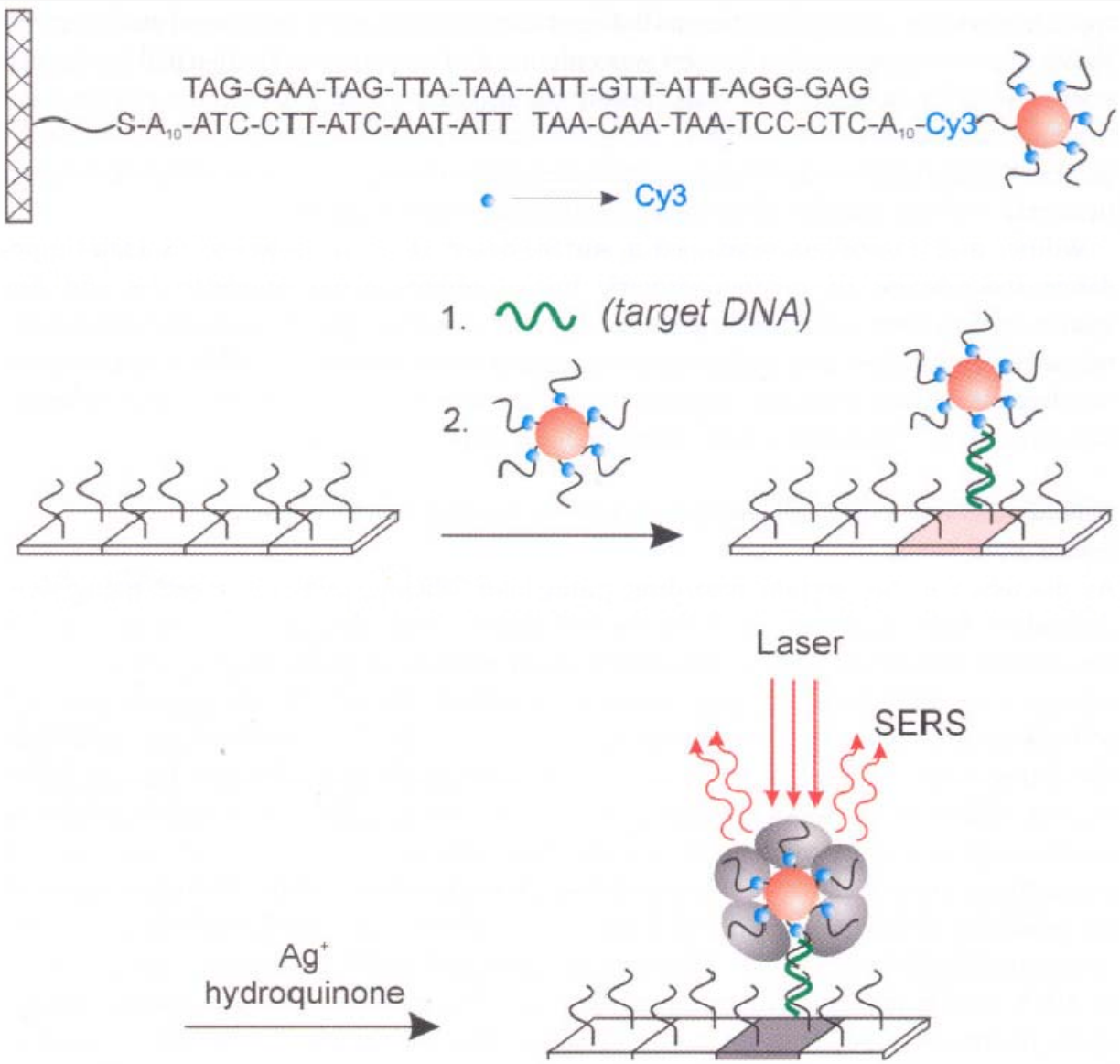


**Figure 19.8** Scheme for surface-enhanced Raman spectroscopic (SERS) detection of DNA targets of interest. In a sandwich assay similar to those above, DNA-nanoparticles encoded with Raman-active dyes (e.g., Cy3) are hybridized to the surface -immobilized capture/target hybrid and silver enhancement is performed. Upon single wavelength laser excitation, the particles emit a strong and reproducible Raman spectrum specific to the Raman-active dye chosen.

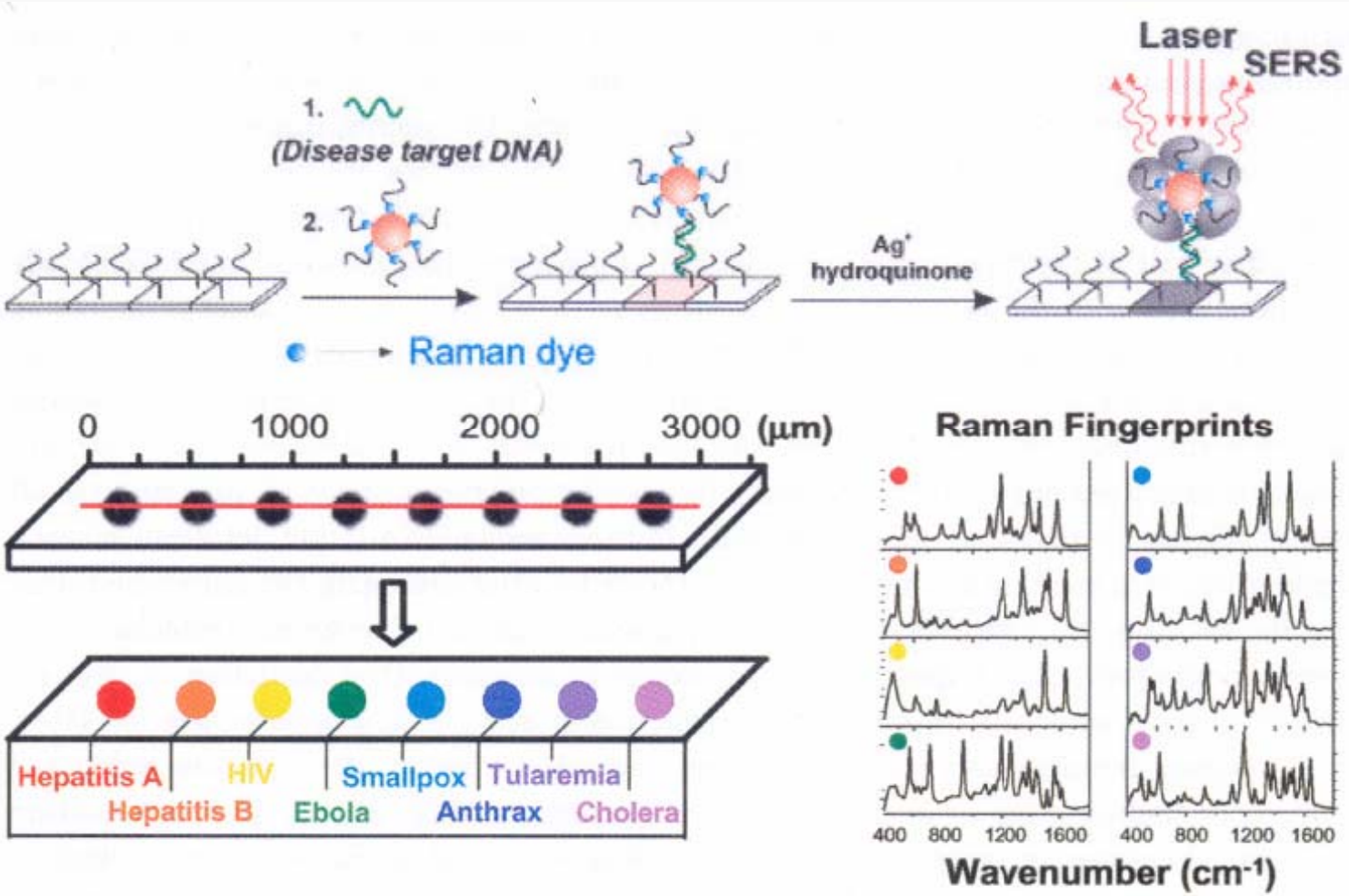


**Figure 19.9** Raman-encoded DNA-nanoparticle detection of multiple DNA targets of interest where each Raman spectrum, or "color" corresponds to a specific target of interest. Here, eight targets were chosen and each assigned a Raman-encoded dye. Note that after silver staining, all of the spots appear black and it is impossible to discern which spot corresponds to which target. However, by using SERS, one is able to scan the spots with a single wavelength excitation laser and observe dye- (and thus, target) specific Raman spectra.

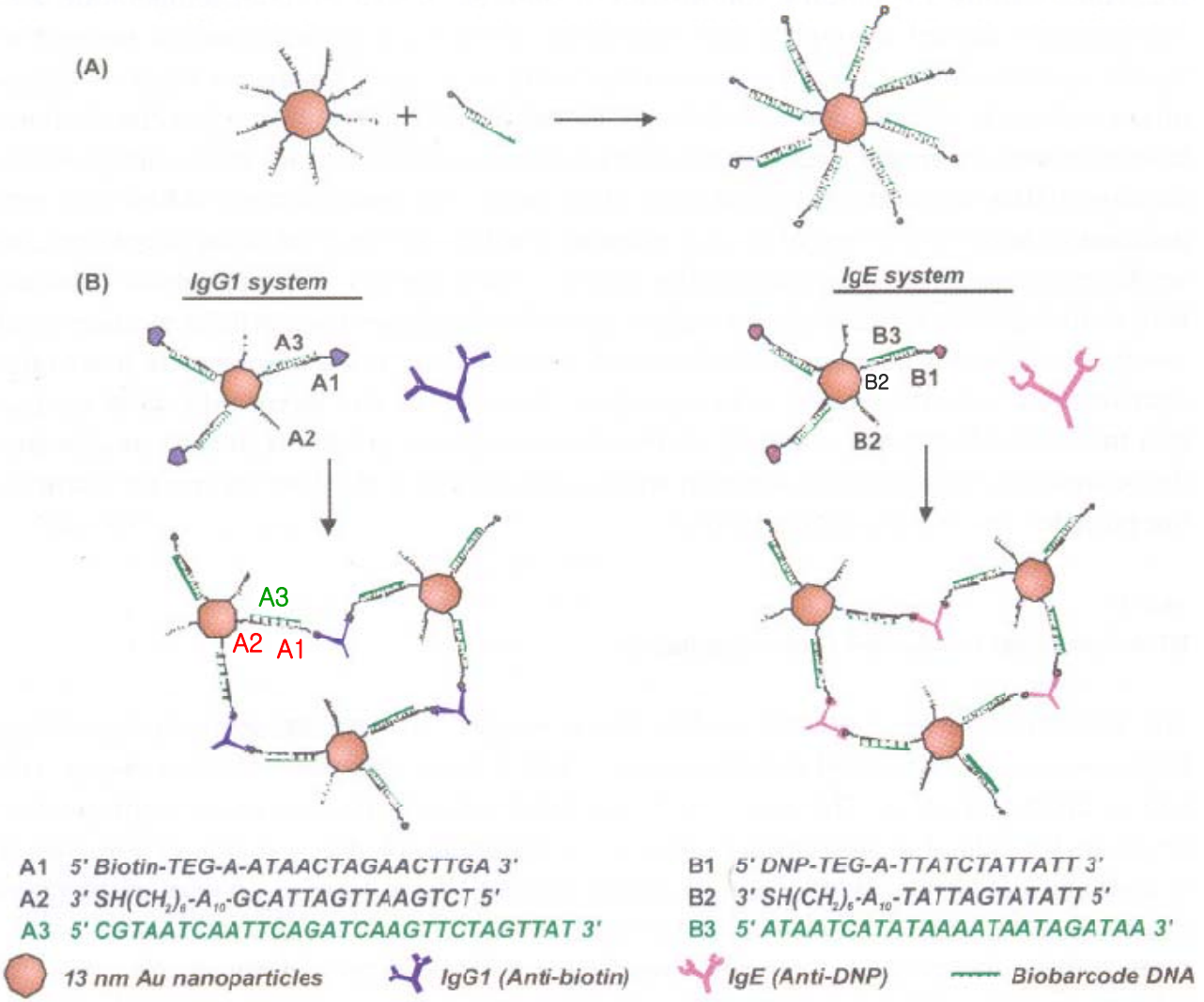


**Figure 19.10** Biobarcode protein detection. (A) Preparation of hapten-modified DNA–Au-NP probes and (B) protein detection using protein binding. Note that there are nine G,C pairs in sequence A, and only two in sequence B; this allows for a large difference in the melting temperature signature that is unique for each protein analyte present.